Research Square

Preprints are preliminary reports that have not undergone peer review.
They should not be considered conclusive, used to inform clinical practice,
or referenced by the media as validated information.

Cataract Surgery via a Surgical Robotic System - First Human Clinical Intervention

Jacob Rosen

jacobrosen@ucla.edu

University of California Los Angeles

Pooria Kashani
Horizon Surgical Systems

Petra Stepke
Horizon Surgical Systems

Peter Ferguson
Horizon Surgical Systems

Changyeob Shin
Horizon Surgical Systems

Alexandre Tiard
Horizon Surgical Systems

Al-Hafeez Dhalla
Horizon Surgical Systems

Mitchell Harris
Horizon Surgical Systems

Eric Peltola
Horizon Surgical Systems

Hai Bui
Horizon Surgical Systems

Hyoenmu Yoo Yoo
Horizon Surgical Systems

David Lozano
UCLA

Uday Devgan
Horizon Surgical Systems

Rajesh Rajpal
Horizon Surgical Systems

Jean-Pierre Hubschman
Horizon Surgical Systems

Steve Schwartz

Horizon Surgical Systems
Richard Lindstrom
Horizon Surgical Systems
Firas Rahhal
Horizon Surgical Systems
Tsu-Chin Tsao
Matt Gerber

Article

Keywords:

Posted Date: August 5th, 2026

DOI: https://doi.org/10.21203/rs.3.rs-9589795/v1

License: This work is licensed under a Creative Commons Attribution 4.0 International License.
Read Full License

Additional Declarations: Yes there is potential Competing Interest. Jacob Rosen – Is a Professor at UCLA and Horizon Surgical Systems Employee Pooria Kashani, Matt Gerber, Petra Stepke, Peter Walker Ferguson, Changyeob Shin, Alexandre Tiard, Al-Hafeez Dhalla, Mitchell Harris, Eric Peltola, Hai Bui, Hyoenmu Yoo, Rajesh Rajpal, Jean-Pierre Hubschman – Are Horizon Surgical Systems Employees Tsu-Chin Tsao - Is a Professor UCLA and a UCLA employee. He is also the Chair of the Scientific board at Horizon Surgical System (Unpaid) David Lozano - Is a Professor at UCLA, a UCLA employee, and a consultant for Horizon Surgical Systems (paid) Steve Schwartz – Is an ophthalmic surgeon in privet practice and a board member at Horizon Surgical Systems (unpaid) Uday Devgan - Is an ophthalmic surgeon in privet practice and a clinical advisory board member at Horizon Surgical Systems (unpaid) Firas Rahhal - Is an ophthalmic surgeon in privet practice and a board member at Horizon Surgical Systems (unpaid) Richard L. Lindstrom - Is an ophthalmic surgeon in privet practice and the head of the clinical advisory board at Horizon Surgical Systems (unpaid)

Cataract Surgery via a Surgical Robotic System - First Human Clinical Intervention

Jacob Rosen[1,2], Pooria Kashani[1], Matt Gerber[1], Petra Stepke[1], Peter Walker Ferguson[1], Changyeob Shin[1], Alexandre Tiard[1], Al-Hafeez Dhalla[1], Mitchell Harris[1], Eric Peltola[1], Hai Bui[1], Hyoenmu Yoo[1], Tsu-Chin Tsao[1,2], David Lozano[1,3], Steve Schwartz[1], Uday Devgan[1], Rajesh Rajpal[1], Firas Rahhal[1], Richard L. Lindstrom[1], Jean-Pierre Hubschman[1]

[1] Horizon Surgical System, Malibu, CA, USA
[2] School of Engineering, University of California Los Angeles (UCLA), LA, CA, USA
[3] School of Medicine, University of California Los Angeles (UCLA), LA, CA, USA

Corresponding Author: Jacob Rosen Ph.D.
Email: jacobrosen@ucla.edu

Abstract

Cataract, characterized by age-related opacification of the crystalline lens, remains the leading cause of global blindness, accounting for approximately 51% of cases worldwide. Advances in surgical robotics, particularly in ophthalmology, are redefining the surgeon's role by integrating autonomous capabilities across sensing, decision-making, and actuation.

This study reports the first robotic-assisted cataract surgeries in humans using the Polaris robotic platform. The system operated in Surgeon Control Mode (SCM) and Surgeon Supervised Mode (SSM), enabling limited autonomous partial nucleus removal. Ten subjects aged 40–75 with visually significant cataracts were randomized; all procedures completed by a single surgeon without intra/postoperative adverse events robotically. At 3 months, UCDVA 20/25 or better achieved in 50% of subjects; three cases of reduced acuity from refractive error were correctable to 20/25 or better. Best-corrected visual acuity reached 20/20 or better in all but two subjects (20/25); surgical step durations in shortest SCM (7:09) were comparable to manual surgery (7:46) in BigCat database.

These results demonstrate that an AI-driven and image guided robotic system, integrating intraoperative OCT with digital microscopy, can safely and effectively execute both surgeon-controlled and partially autonomous surgical tasks while maintaining the precision and accuracy required for ophthalmic procedures. More broadly, the introduction of autonomy in surgical robotics has the potential to transform the three foundational pillars of surgery: enhancing surgeon capabilities through improved sensing, cognition, and actuation; improving patient outcomes and access to care; and increasing healthcare system efficiency to address the growing disparity between surgical demand and workforce capacity.

1. Introduction

Cataract, the age-related opacification of the crystalline lens, remains a major cause of visual impairment, accounting for 51% of global blindness. Distribution ranges as low as 5% in developed countries and over 50% in regions like sub-Saharan Africa and Asia. The most common treatment is the surgical removal of the opacified lens by phacoemulsification, in which ultrasonic energy fragments the lens and the material is aspirated, followed by implantation of an intraocular lens (IOL) to restore optical function. [1,2,3]

Cataract extraction with intraocular lens implantation is one of the most commonly performed surgeries in ophthalmology, and the total number of cases worldwide have more than doubled in recent decades, rising from about 32.8 million in 1990 to 82.2 million in 2021, and are projected to continue increasing under current demographic trends, making it one of the highest-volume surgical interventions across the healthcare systems.

The global burden of cataract continues to rise, primarily due to population growth and increased life expectancy, with absolute numbers of cataract cases increasing substantially despite some regional improvements in age-standardized visual impairment rates. [3]

Minimally invasive cataract surgery, primarily phacoemulsification, revolutionized eye care by replacing open, large-incision techniques with two small, self-sealing incisions (approximately 2.2–2.8 mm for the main incision and 0.9–1.2 mm for the side incision). Compared to historical "open" methods, this approach offers faster recovery, reduced complications, and improved vision outcomes, allowing the procedure to be performed in an outpatient setting[4-6]

Despite these favorable clinical outcomes with increasingly minimally invasive and predictable surgical techniques, cataract surgery still carries a risk of complications that are potentially vision-threatening. Posterior capsule rupture (PCR), with or without vitreous loss, is the most commonly studied intraoperative adverse event, with reported incidence ranging from approximately 0.7 % to 1.9 % in large clinical audits and national cohort analyses. [7,8] Other significant complications in otherwise-typical eyes can occur at rates of 0.5-2%, including zonular dialysis 0.5% [39], corneal endothelial decompensation 1-2% [40], sustained elevated intraocular pressure 2 to 8% [41], cystoid macular edema 1-2% [42], and, rarely, infectious endophthalmitis <1% .[4–6,9] These events can prolong recovery, reduce visual prognosis, and increase the need for secondary interventions when they occur.

Given the large volume of cataract procedures, even infrequent complications can have an extensive impact on patient outcomes and health-care burden. Therefore strong impetus remains to explore technologies that can improve surgical accuracy, precision, and reliability.

However, these improvements are fundamentally constrained by the inherent physiological limitations of the human surgeon, including hand tremor and sensory thresholds that challenge microscale intraocular manipulation and repeated execution of highly delicate steps, such as capsulorhexis and nucleus disassembly and removal under microscopic visualization [10] .

Surgical robotics, as introduced into the operating room (OR), is fundamentally predicated on two core capabilities: (1) enhanced dexterity, accuracy, and precision in positioning, orienting, and manipulating anatomical structures relative to conventional handheld instruments, and (2) improved visualization through the integration of multimodal imaging technologies [11-13]. Early implementations of surgical robotic systems primarily addressed procedures involving soft tissues—characterized as unstructured, dynamic, and nonlinear viscoelastic environments—such as those encountered in abdominal and thoracic surgery. In these contexts, direct preoperative trajectory planning was infeasible due to intraoperative tissue deformation and variability. Consequently, teleoperation emerged as the dominant control paradigm, wherein the surgeon operates from a console and provides real-time position and orientation commands via master input devices, which are translated into precise movements of robotic instruments at the patient side [11,14-16].

In contrast, applications involving hard tissues—considered structured environments—such as in orthopedic surgery, enabled a different paradigm of human–robot interaction. While maintaining surgeon involvement, these systems often eliminated the need for a remote console and instead employed cooperative or hands-on control schemes. In such configurations, the surgeon directly manipulates the robotic arm or end effector, with the robotic system enforcing constraints through virtual fixtures derived from preoperative imaging and planning [17,18]. These virtual fixtures guide bone resection or implant placement by restricting tool motion to predefined safe regions, enabled by accurate registration between preoperative scans and the patient anatomy [18].

Despite the predominance of surgeon-in-the-loop control architectures, automation has remained the central overarching goal of surgical robotics. The feasibility of automation depends on satisfying one of two conditions: (1) the presence of a structured environment, in which anatomical geometry can be accurately captured preoperatively, allowing for trajectory planning and execution under the assumption of spatial stability; or (2) the availability of real-time intraoperative imaging modalities—such as ultrasound or optical coherence tomography (OCT)—capable of continuously updating anatomical models and enabling adaptive trajectory planning in response to tissue deformation [19].

The eye represents a unique hybrid case within this framework. Although composed predominantly of soft tissues, the maintenance of intraocular pressure (IOP) during ophthalmic procedures provides a quasi-stable environment that can approximate the characteristics of a structured domain. This property enables partial reliance on preoperative planning while still necessitating intraoperative adaptability. Furthermore, the integration of high-resolution, real-time imaging modalities—particularly OCT co-registered with surgical microscopy or digital video—allows for continuous monitoring of tissue-tool

interactions and dynamic updating of surgical trajectories [20]. These capabilities position ophthalmic surgery as a compelling domain for advancing semi-autonomous and fully autonomous robotic interventions.

Research has driven the development of various ophthalmic robotic systems [10, 21-24], ranging from handheld tremor-suppressing instruments [25] to cooperative 'steady-hand' robots [26]. Notable among these are two generations of the Intraocular Robotic Interventional and Surgical System (IRISS). This system enables tele-operated, image-guided (OCT and digital microscopy) [43-45], and AI-driven automated surgery for both anterior (e.g., cataract) and posterior (e.g., vitreoretinal) procedures, incorporating force feedback and tissue detection [27-35]. Experimental and preclinical studies have demonstrated that robotic systems can reduce tool-tip motion and enable complex tasks such as retinal vein cannulation and subretinal injection, which are challenging or infeasible with manual techniques alone.

Robotic systems in ophthalmology have recently transitioned from experimental prototypes to clinical application, demonstrating safety and feasibility in human patients. The Preceyes Surgical System (Preceyes BV / Carl Zeiss Meditec) was used in first-in-human studies (2018) to assist retinal surgery, including epiretinal and internal limiting membrane peeling, showing that telemanipulation enables precise intraocular movements under both local and general anesthesia [36]. Subsequent trials (2022) have applied robotic assistance to subretinal drug delivery in patients with macular degeneration, highlighting the system's potential for high-precision therapeutic interventions [37]. The Luca system (AcuSurgical) is a bi-manual surgical robotic system was utilized to perform first in human vitreoretinal surgery (2024) [38]

This paper presents the world first-in-human study, conducted in October 2025, of the Polaris (Horizon Surgical Systems), a robotic platform for cataract surgery. The system was used to assist phacoemulsification procedures, and its performance was evaluated through analysis of operative parameters, safety outcomes, and early performance metrics in the context of existing literature. Evaluation criteria included safety, effectiveness, workflow integration, and early clinical outcomes. The results highlight key opportunities and challenges for broader adoption in ophthalmic practice.

2. **Methods**
a. **Surgical Robotics System**

Polaris by Horizon Surgical Systems is a surgical robotic platform designed specifically for ophthalmology (Figure 1). Its development is based in part on extensive academic research efforts [27-35] prior to an ongoing commercialization effort by Horizon Surgical System since 2022. The surgical robotic system (Polaris) comprises two primary subsystems: (1) the surgical cart, which interfaces with the patient, and (2) the surgical cockpit, which interfaces with the surgeon.

The surgical cart is a cluster of subsystems, including an imaging head that acquires

multimodal visual information from the patient's eye, and a robotic system that manipulates surgical instruments within and external to the patient's eye.

The imaging head integrates four imaging channels and multiple illumination systems. In addition to oblique illumination (main lamp), co-axial illumination (red reflex), and stereomicroscopy common to all modern ophthalmic surgical microscope platforms, the imaging head adds two additional telecentric imaging channels: a third microscopy channel centered on the common main objective, and a Swept-Source Optical Coherence Tomography (OCT) channel, co-axial and co-registered with the telecentric microscopy channel.

This visualization head is connected to the cart frame via a Cartesian XYZ robotic system, enabling positioning of the imaging head relative to the patient's eye. A large-form-factor 6DOF Macro robotic arm, responsible for gross manipulation, is attached to the surgical cart frame and manipulates a small-form-factor 5 DOF micro robotic arm with a remote center of motion (RCM), which is responsible for the fine manipulation of surgical instruments. A set of Interchangeable surgical instruments are attached to the micro manipulator by a nurse via a universal interface, which allows for additional actuation for specific surgical instruments by the Micro arm. A surgical sterile drape covers both surgical robotic arms (Micro and Macro) using a sterile barrier that is established at the universal interface of the Micro robotic arm. The surgical procedure is conducted under the assumption that the eye remains sufficiently stable throughout the procedure. A docking ring is physically attached to the imaging head via a stem while restraining the eye in space via a suction cup. A wheeled frame houses the system's computers and provides sufficient rigidity to support the accuracy and precision required for ophthalmic procedures.

The surgical cockpit encompasses all input/output devices that enable the surgeon to perceive visual information and to manipulate and actuate the surgical instruments. A joystick is used to control the position of the Macro robotic arm allowing the surgeon to position the RCM at the corneal incision. A 5 DOF input device is held by the surgeon's hand and used to provide input commands to the Micro robotic arm allowing the surgeon to control the surgical tool outside and inside the eye including insertion through the corneal incision during the Surgeon-Supervised Mode (SSM). Additional input 3 DOF input device allows the surgeon to control the cartesian position of the imaging head with respect to the patient eye. A stereoscopic view of the patient's eye along with OCT view of the patient's eye, allowing the surgeon to select a specific cross section, are acquired by the imaging system and displayed on a 3D screen included in the surgical cockpit. Additional control of the system is provided to the surgeon via two foot pedals: a phacoemulsification footswitch (Alcon CENTURION) and a customized foot pedal to control robotic motion, illumination settings, and microscope focus and pan.

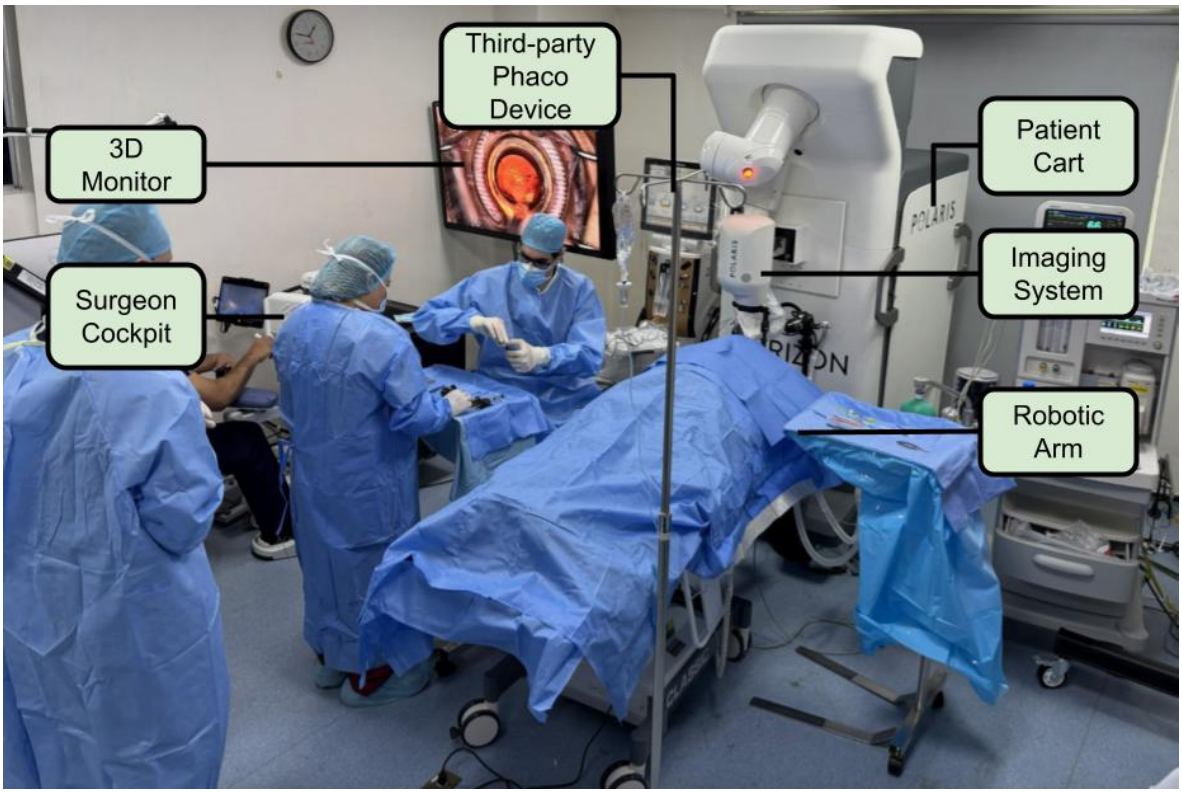


Figure1: Overview of the Polaris Surgical System setup at the operating room during the first in human study.

b. **Modes of Operation**

The Polaris system was operated in one of two modes: Surgeon-Controlled Mode (SCM) and Surgeon-Supervised Mode (SSM).

In SCM, the surgeon performed surgical tasks using input devices and foot pedals within the surgeon cockpit. Surgeon hand movements were mapped to instrument motion using predefined scaling factors, and the system provided visual feedback through a 3D stereoscopic display.

In SSM, the Polaris system automatically acquired visual data of the eye, identified anatomical features of interest within that data via trained AI based segmentation models, and generated a surgical plan for execution of the surgical step. The surgical plan included an instrument trajectory and actuation sequences. The surgeon reviewed the workspace and trajectory, modified them if necessary, and provided approval. The Polaris system then executed the plan by controlling instrument motion and irrigation, aspiration, and ultrasound functions, while continuously monitoring the surgical workspace for anatomical deviations beyond predefined thresholds. If such deviations were detected, a safe stop could be automatically triggered. Throughout SSM execution, the surgeon supervised the procedure and retained the ability to intervene, pause, or assume control through SCM.

c. Study Design and Experimental Protocol

I. Study Design Overview and Sample Population

The objective of the study was to assess the safety and efficacy of using the Polaris System in cataract surgery. This was a single-center study with non-randomized and non-masked treatments on 10 subjects using the same robotic system. The primary safety endpoint was the rate of ocular adverse events during the study. Clinical performance endpoints included uncorrected distance visual acuity (UCDVA) and best-corrected distance visual acuity (BCDVA) at all visits. The target study population comprised adults (male or female) aged 40–75 years (inclusive) with a slit-lamp diagnosis of visually significant, uncomplicated, age-related cataract (excluding posterior polar and congenital cataracts). Subjects were considered enrolled upon giving written informed consent. After unilateral cataract surgery, subjects were evaluated through 3 months of postoperative follow-up.

II. Subject Eligibility

Consenting male or female patients aged 40 to 75 years diagnosed with visually significant age-related cataract and planning to undergo surgical treatment with IOL implantation were eligible to participate in the study.

Patients with previous ocular surgery, contraindication to any medication, anticipated difficulty with a planned procedure/assessment or otherwise presented with or had a history of a condition or disease that could increase surgical risk or otherwise confound study outcomes were to be excluded from study participation

III. Surgeon Experience and Training

A trained cataract surgeon (Investigator) with 25 years of experience after residency and formal surgical training performed all 10 cases in this study. The surgeon also completed system-specific training, which included cataract procedures on porcine eyes and human cadaver eyes;.

IV. Surgical Protocol

Prior to the robotic surgical procedures included in the study, subjects underwent continuous curvilinear capsulotomy via femtosecond laser platform (LENSAR). Following eye preparation, docking was engaged to the patient eye, and viscoelastic was applied to enhance visualization and protect the corneal epithelium. The Polaris was then transitioned into SCM, and the surgical steps defined in Table 2 were performed in

sequence. Nucleus extraction was performed exclusively in SCM cases while partial nucleus extraction and nucleus removal completion were performed exclusively in SSM+SCM cases. Wound ~~closure~~ hydration and IOP checks were performed by the assistant surgeon following IOL positioning and OVD removal.

For cases utilizing SSM, a surgical plan for performing partial nucleus extraction was generated and presented for surgeon review. Upon surgeon confirmation, the plan was autonomously executed by the system. After stopping SSM execution, the system was transitioned back to SCM, and the surgeon completed the remaining nucleus extraction using SCM controls.

Five out of ten patients received treatment via SCM for all surgical steps (i.e., no SSM was used) while the remainder received treatment with SSM for partial nucleus extraction and SCM for all other surgical steps.

V. **Clinical Outcome Measures**

Each eye was post-operatively assessed via slit-lamp biomicroscopy, tonometry, and fundus examination. Vision performance was assessed with and without best correction for distance. Clinical assessments were conducted postoperatively at 1 day, 1 week, 1 month and 3 months.

VI. Operational Time Analysis

Video footage collected during the study was analyzed to investigate the distribution of time durations for various surgical steps using the Polaris system (**Table 1**).

Surgical Step (Abbreviation)	Operational Definition
Main Incision (INC)	Start - Incising the cornea using the micro arm of the Polaris system End - Fully extracting the keratome from the eye
Hydrodissection (HYD)	Start - Inserting the hydrodissection cannula into the anterior chamber of the eye End - Fully extracting the hydrodissection cannula from the eye
OVD Injection (VIS) (Alcon Viscoat)	Start - Inserting the Viscoat cannula into the anterior chamber of the eye End - Fully extracting the Viscoat cannula from the eye
Nucleus Extraction (NE-SCM)	Start - Inserting the phacoemulsification handpiece into the anterior chamber of the eye End - Fully extracting the phacoemulsification handpiece from the eye *note: this step is exclusive to SCM cases
Partial Nucleus Extraction (PNE-SSM)	Start - Initiating SSM lens bowl planning End - SSM lens bowling operations ceased at the discretion of the primary surgeon *note: this step is exclusive to SSM+SCM cases
Nucleus Removal Completion (NRC)	Start- Transitioning the Polaris system to SCM for the completion of nucleus removal following SSM partial nucleus extraction End - Fully extracting the phacoemulsification handpiece from the eye *note: this step is exclusive to SSM+SCM cases
Cortical Material Removal (CMR)	Start - Inserting the I/A handpiece into the anterior chamber of the eye End - Fully extracting the I/A handpiece from the eye
OVD Injection (PRO) (Alcon Provisc)	Start - Inserting the Provisc cannula into the anterior chamber of the eye End - Fully extracting the Provisc cannula from the eye
IOL Injection (IOL)	Start - Inserting the IOL cartridge into the anterior chamber of the eye End - Fully extracting the IOL cartridge from the eye
OVD Removal (OVD) - Including IOL Positing	Start - Inserting the I/A handpiece into the anterior chamber of the eye End - Fully extracting the I/A handpiece from the eye

Table 1: Operational Definitions and Abbreviations of the Surgical Steps Performed by the Polaris System.

3. Results

a. Subject Accountability & Demography

A total of 14 subjects gave written consent to participate in the study, 12 of whom met the preoperative eligibility criteria. Two subjects withdrew prior to surgery due to illness or transportation difficulties, and 10 subjects successfully completed unilateral surgery on the study eye (Table 2). The 10 treated subjects ranged from 52 to 71 years of age, with a mean age of 62.8 years. Subjects were randomly assigned to one of the two treatment groups based on the two operational modes of the surgical robotic system including: (1) SCM and (2) SCM + SSM (see section 2.c.IV)

Subject Number	Group	Gender / Age
101	SCM+SSM	Female / 68
103	SCM+SSM	Female / 64
104	SCM	Male / 71
106	SCM	Male / 69
107	SCM	Female / 52
109	SCM+SSM	Female / 55
110	SCM	Female / 64
111	SCM+SSM	Female / 61
112	SCM	Female / 64
114	SCM+SSM	Female / 60

Table 2: Subjects listed by assigned treatment group, demographic, and cataract LOCS III grading

b. Operational Summary

The study investigator successfully completed surgery in all 10 cases using the Polaris system. There were no conversions from Polaris-assisted to manual procedure, and no surgical complications or adverse events occurred in the study. One observation was noted for a subject whose facial anatomy (nose) challenged surgical access, but the surgery for this subject was completed uneventfully.

c. Postoperative Outcomes

i. Intraocular Pressure (IOP)

At Day 1 postoperative, there were no adverse events, including IOP spike, and all subjects had uncorrected visual acuities of 20/55 or better (Snellen equivalent). Slit lamp findings were typical for the immediate postoperative period, including low- to moderate-grade corneal edema, conjunctival injection, and cells and flare at the Day 1 visit. All findings were reported to be within normal limits by the Day 7 visit. Ocular surface

dysfunction and one report of dry age-related macular degeneration were noted postoperatively.

ii. Uncorrected Visual Acuity (UCDVA)

Uncorrected visual acuity (UCDVA) was generally stable throughout the postoperative period, improving or remaining unchanged for most subjects at subsequent study visits (Figure 2). At the Month 3 visit, UCDVA was 20/25 or better for half of the subjects. Two subjects had UCDVA of 20/40 due to residual refractive error (both correctable to 20/25), including one subject with a 2-line decrease from the previous visit, attributed to dry eye. One subject had UCDVA of 20/50 due to residual refractive error (correctable to 20/16).

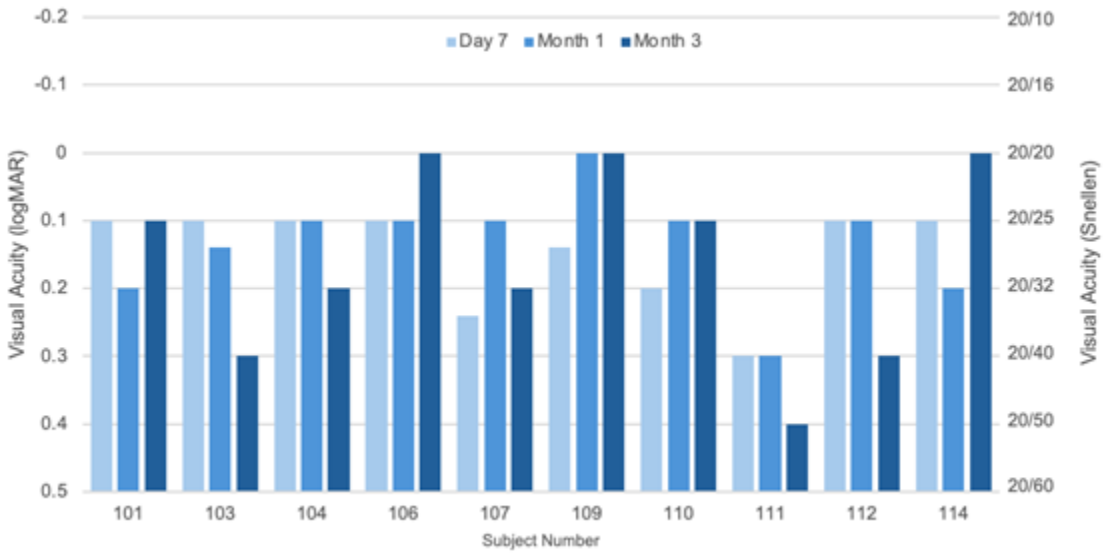


Figure 2: Uncorrected Distance Visual Acuity (UCDVA) over time

iii. Best-corrected distance visual acuity (BCDVA)

Best-corrected distance visual acuity (BCDVA) at Day 7 was 20/20 for all subjects except one (20/25), and visual acuities were relatively stable through the postoperative period (Figure 3 and Table 3). Two subjects had BCDVA that decreased from Day 7 to the Month 1 but still 20/28 or better. By the Month 3 visit, visual acuity was unchanged or improved for 9 of 10 subjects; nearly all subjects had BCDVA of 20/20 or better, except for two subjects with 20/25 BCDVA.

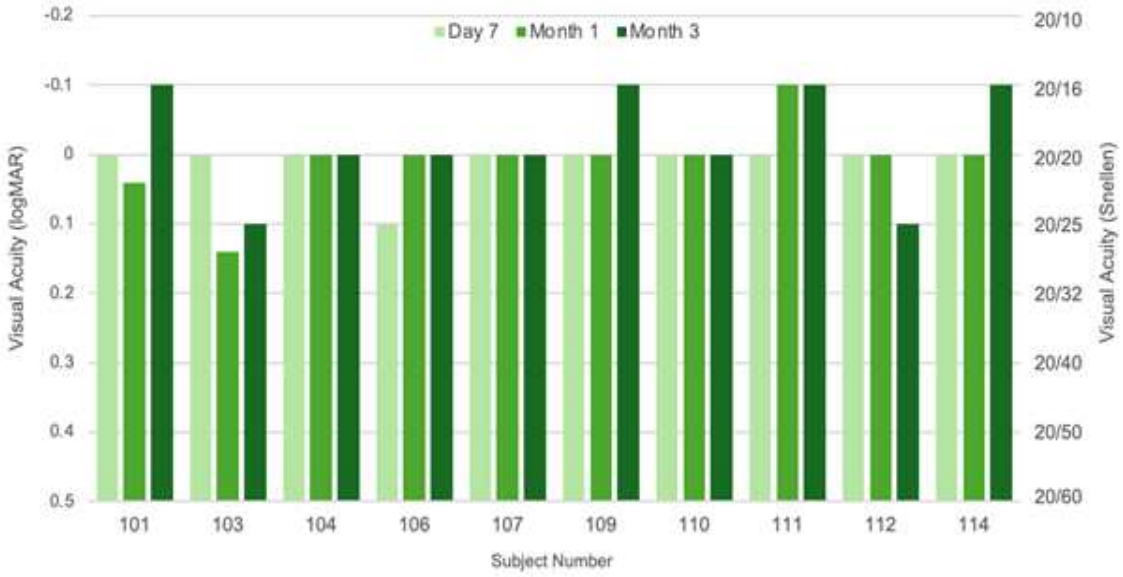


Figure 3: Best Corrected Distance Visual Acuity (BCDVA) over time

Subject Number	BCDVA change from Day 7 to Month 1	BCDVA change from Month 1 to Month 3
101	Decreased 2 letters	Improved 1.5 lines
103	Decreased 1.5 lines	Improved 2 letters
104	Stable	Stable
106	Improved 1 line	Stable
107	Stable	Stable
109	Stable	Improved 1 line
110	Stable	Stable
111	Improved 1 line	Stable
112	Stable	Decreased 1 line
114	Stable	Improved 1 line

Table 3: BCDVA Outcomes

d. Intraoperative OCT B-Scan Analysis

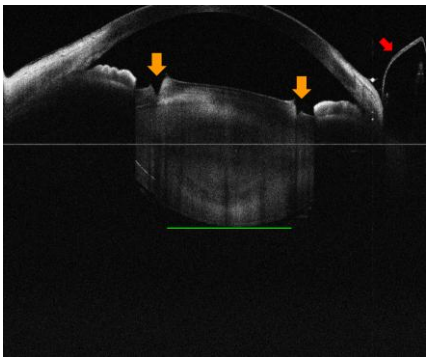
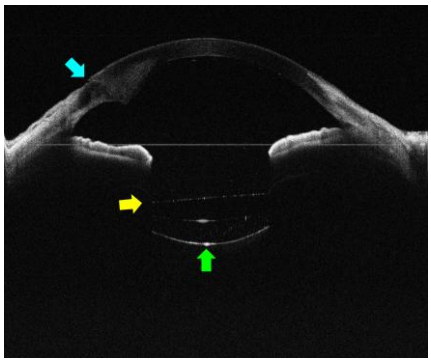
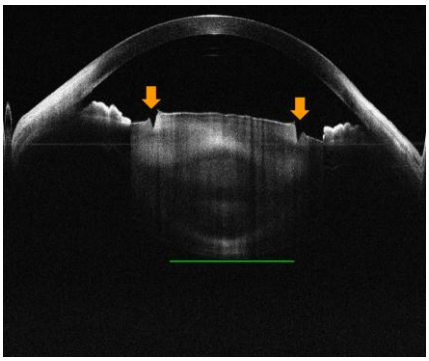
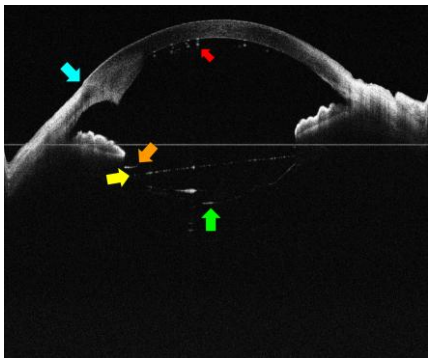
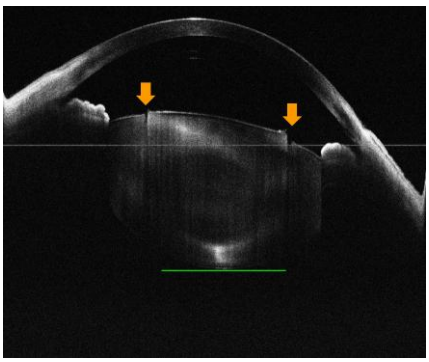
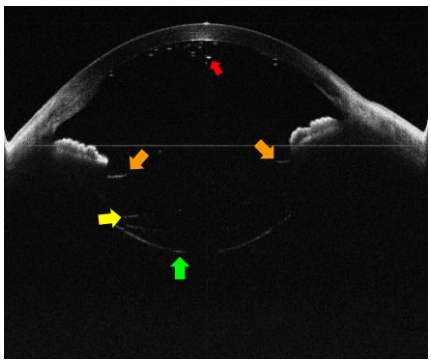
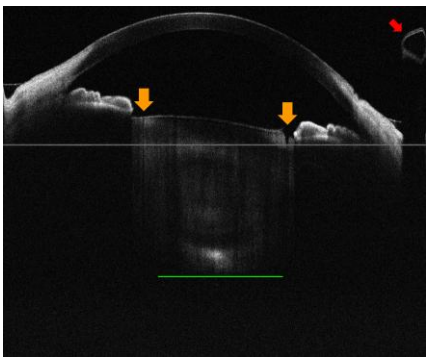
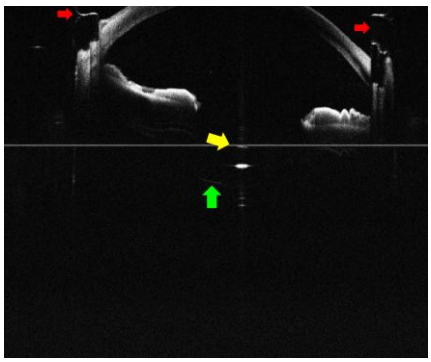
Intraoperative OCT B-scans acquired for each subject are presented in Figure 4. All B-scans are composite images generated by averaging three consecutive frames (±1 adjacent frames) from the volumetric OCT data. Pre-manual preparation scans were acquired after capsulotomy but prior to manual preparation steps (i.e., they were acquired prior to making any surgical incision in the eye). Pre-speculum removal scans were acquired after completion of all manual closure steps, immediately prior to speculum removal.

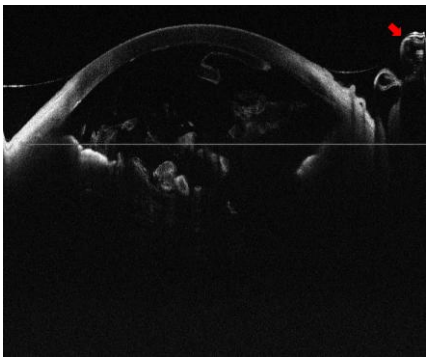
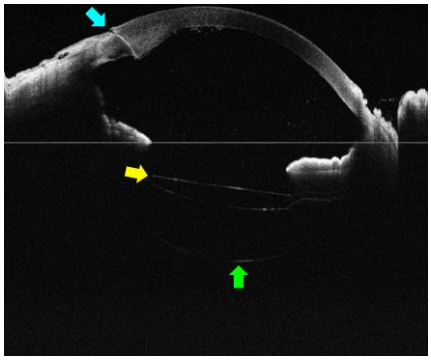
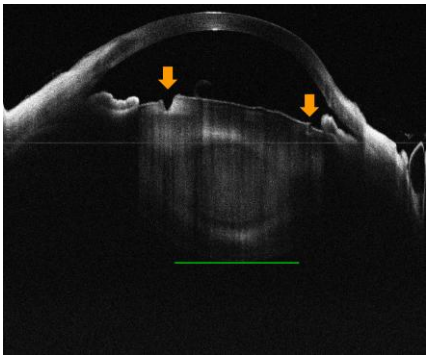
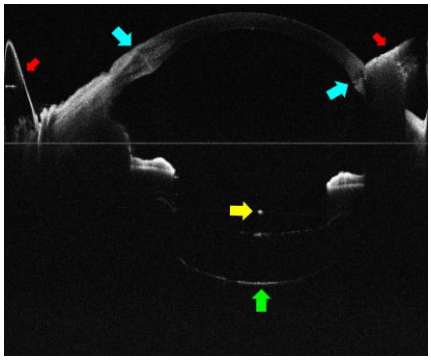
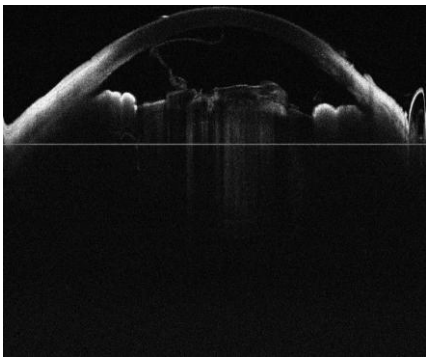
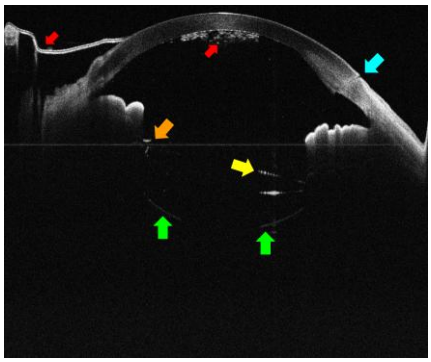
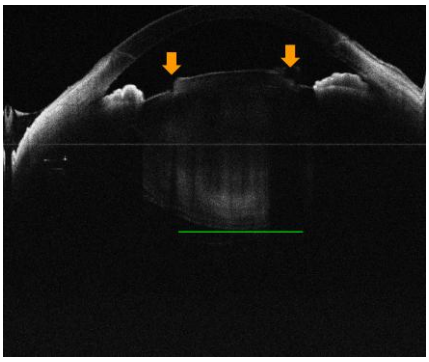
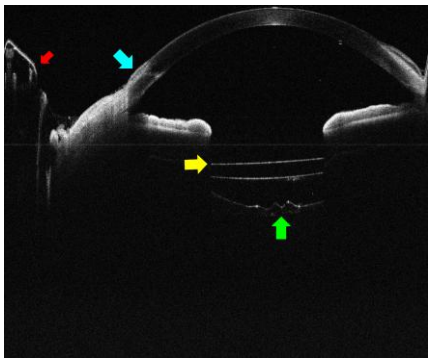
Exceptions to these acquisition timepoints include subjects 103 and 104, whose pre-manual preparation scans were acquired during manual preparation procedures (later than intended), and subject 106, whose pre-speculum removal scan was acquired prior to manual closure steps (sooner than intended). These scans were not acquired at the prespecified timepoints due to competing intraoperative priorities and efforts to minimize disruption to the surgical workflow.

Aside from the aforementioned exceptions, all pre-manual preparation scans demonstrate the capsulotomy created by the femtosecond laser but are otherwise unremarkable.

In all pre-speculum removal scans, the intraocular lens (IOL) and posterior capsule (PC) are visible, demonstrating that the PC is intact and the IOL is centered within the eye. Furthermore, in subjects 112, 110, and 103, portions of the anterior chamber are visible, supporting the interpretation that the IOL is contained within the capsular bag. However, in many scans (particularly those from subjects 110, 103, 114, and 109) the presence of air bubbles in the anterior chamber (accumulating along the corneal endothelium) severely degrades OCT image quality, limiting visualization of the IOL and PC. Variability in OCT liquid lens scanning depth (laser focus) also contributed to suboptimal visualization of the IOL and PC in many cases.

The extent of the retro-IOL space observed in each subject is consistent with intraoperative OCT findings from cadaver eye studies acquired immediately following OVD removal, in which the PC does not immediately collapse and conform to the IOL optic. The retro-IOL spaces are generally uniform and symmetric, and the PC demonstrates a smooth, posteriorly convex contour. Subject 111 demonstrates a wavy PC contour, which may reflect reduced IOP and/or anterior chamber underinflation; the relatively shallow capsular bag observed in this scan is consistent with this interpretation.

Subject ID	Pre-manual Preparation OCT B-scans	Pre-speculum Removal OCT B-scans
107 SCM		
112 SCM		
110 SCM		
106 SCM		

104 **SCM**		
101 **SCM+SSM**		
103 **SCM+SSM**		
111 **SCM+SSM**		

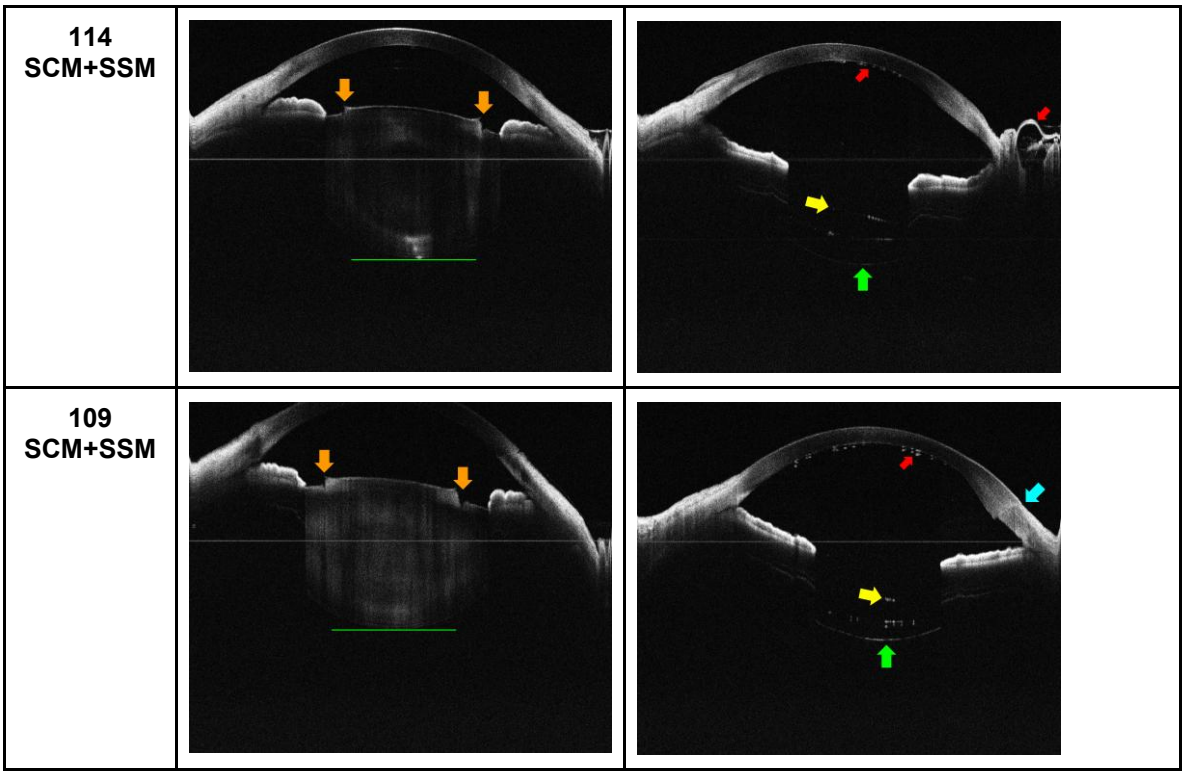
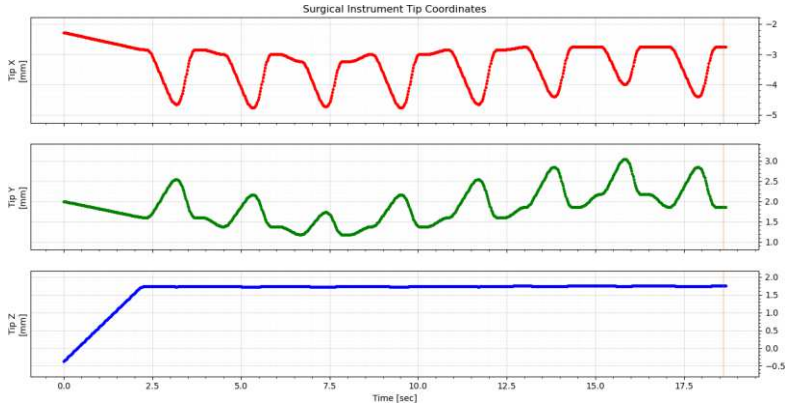


Figure 4 - OCT B-scans acquired for each subject prior to manual preparation steps and prior to speculum removal. Orange arrows (in pre-manual preparation scans): femtosecond laser–created cuts in the anterior chamber; Orange arrows (in pre-speculum removal scans) anterior capsule (when visible); Green line: posterior-most extent of the posterior capsule; Yellow arrow: anterior surface of the intraocular lens (IOL) optic; Green arrow: posterior capsule; and Cyan arrows: corneal incisions (when visible). Small red arrows indicate intraoperative obscurants, including air bubbles in the anterior chamber, surgical drape intrusion, and a Weck-Cel sponge. Not indicated are OCT acquisition artifacts, including mirror (complex conjugate) artifacts (most apparent in the iris); dual-edge sampling artifacts (manifesting as a high-intensity horizontal line); and signal saturation (particularly at the IOL apex).

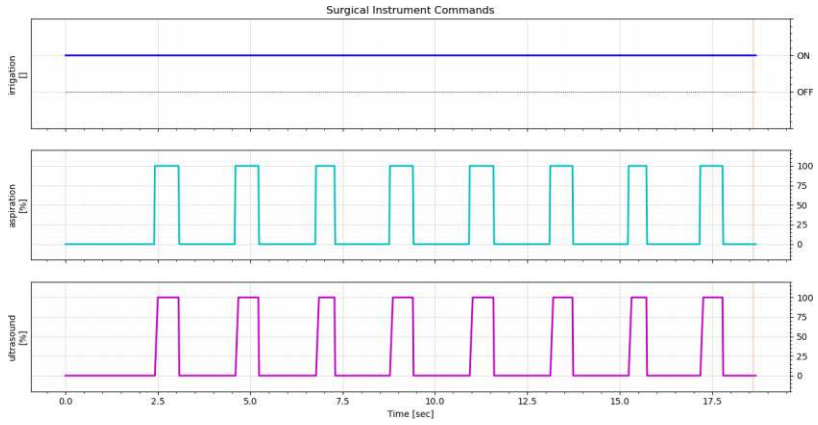
e. Surgeon Supervised Mode (SSM)

Using Subject 101 as an illustrative example, the trajectory planning and execution framework is described as follows. Figure 5a shows the decomposition of the initial trajectory for Subject 101 into Cartesian coordinates, while Figure 5b presents the corresponding commanded system parameters. Although a complete trajectory plan is generated, in practice only the initial portion (typically the first petal) is executed before automatic adjustment occurs. After approximately 1.5 seconds of trajectory execution (corresponding to roughly half of a forward pass) new OCT data is acquired and processed, and an updated trajectory is generated based on anatomical changes.

To maintain procedural efficiency, OCT data are continuously analyzed to estimate the depth and spatial distribution of remaining lens material. The trajectory generator uses this information, along with the current system state, to determine whether an update to the active trajectory is required and, if so, how to modify it (i.e., where to move the instrument next). This decision primarily concerns the appropriate depth and lateral location for the next pass. Once computed, the updated trajectory is transmitted to the robotic controller for execution.



(a)



(b)

Figure 5 - Trajectory generation and execution during SSM of partial nucleus extraction of subject no. 101 (a) Time-series representation of the instrument-tip trajectory decomposed into X, Y, and Z components in the robot base frame. (b) Time-series representation of the instrument commands (irrigation, aspiration, and ultrasound) for the initial trajectory plan.

Figure 6 shows an annotated OCT B-scan cross-section of the eye immediately following successful autonomous, image-guided partial nucleus extraction in Subject 101. The green arrow indicates the region of completed nucleus extraction, extending to approximately 40% of the lens depth. The yellow arrow denotes the posterior capsule; note that hydrodissection was performed prior to this step, and separation between cortical material and the nucleus is clearly distinguishable. The red arrow highlights cortical material that has prolapsed from the capsular bag into the anterior chamber, as is typical.

The fine linear feature observed in the upper-right region of the anterior chamber (cyan arrow) does not represent Descemet's membrane detachment; rather, it corresponds to a retained anterior capsule lenticule from the femtosecond laser capsulotomy, which was not removed by the surgeon until after completion of the SSM step.

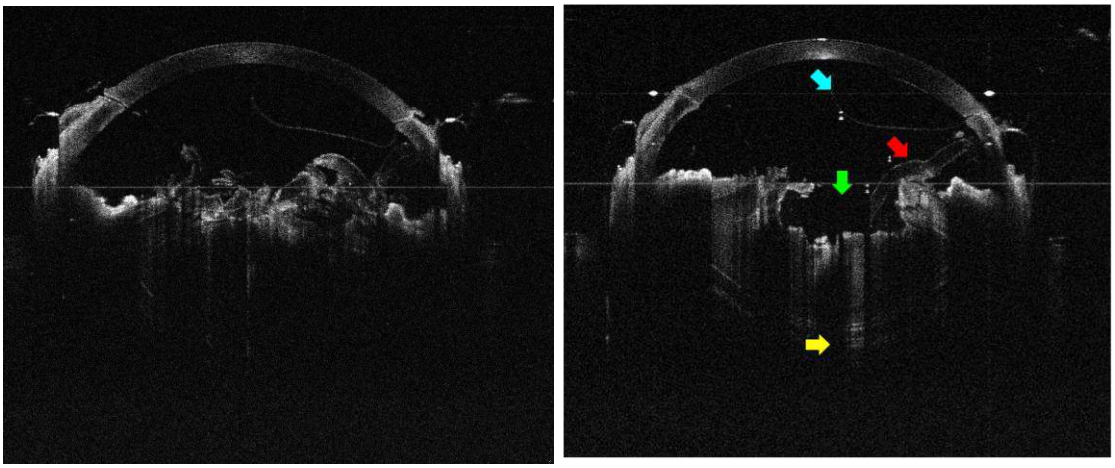


Figure 6: OCT B-scans acquired (a) before and (b) after SSM-performed partial nucleus extraction. The arrows follow the following color scheme: Cyan: retained AC lenticle/flap (not DMR); Red: lens cortex; Green: partially extracted nucleus; Yellow: PC (plus hydro cleaving planes anterior to it).

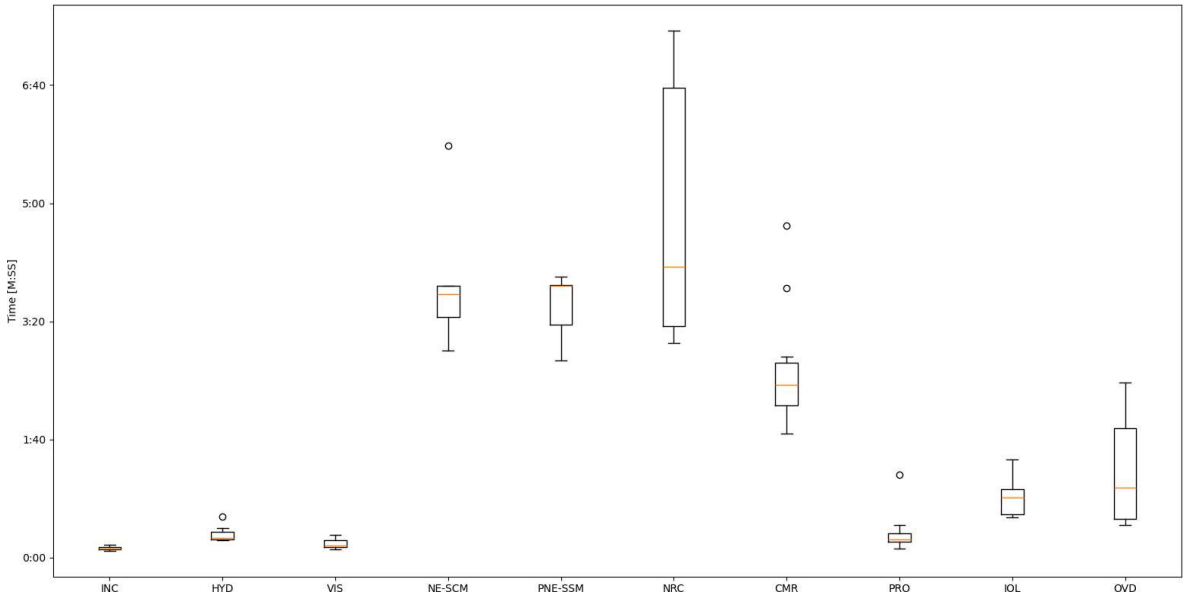
f. Operational Time Analysis

The durations of individual surgical steps (Table 2) were analyzed to assess trends across the clinical trial. Figure 7a presents box plots summarizing the statistical distribution of the various step time durations. The same data are presented as a percentage of each one of the cases (SCM and SCM-SSM) in Figure 7b. As expected, INC, HYD, VIS, and PRO were the shortest surgical steps with mean operative time of 8.2 ± 1.5 s, 19.6 ± 6.1 s, 11.9 ± 3.9 s, and 21.7 ± 16.9 s, respectively. IOL and OVD took 50.8 ± 14.8 s and 74.3 ± 45.6 s. CMR time was 159.7 ± 52.1 s. The SCM-performed phacoemulsification step (NE-SCM) took 236.2 ± 59.5 s while the same step with SSM took over twice as long: the SSM portion (PNE-SSM) took 212.6 ± 26.9 s and the SCM portion (CMR) took 293.6 ± 108.0 s.

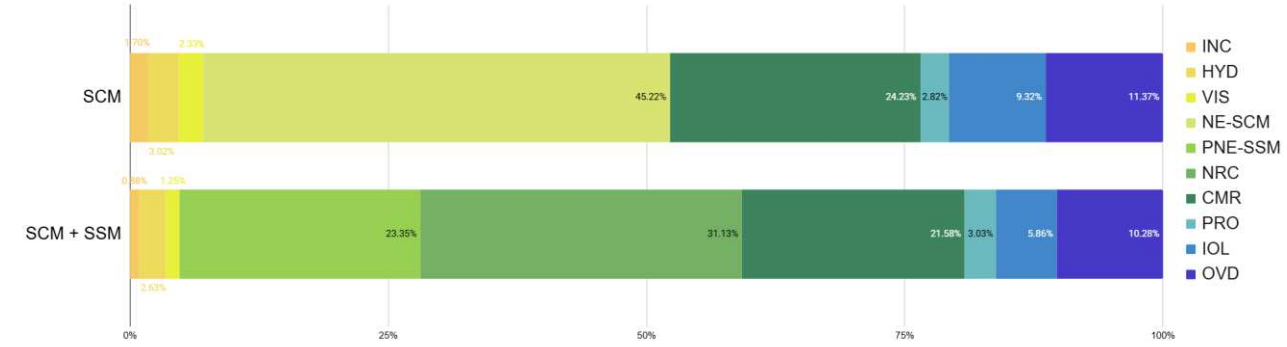
The shortest case using SCM (Subject 110) was compared to the data available in the BigCat database on average surgical step durations (Figure 7c). The identified equivalent surgical steps across both studies are presented in table 5. The total surgical durations calculated for the shortest SCM case and an equivalent manual surgery are 7:09 and 7:46 [38] respectively, including the following steps: INC, HYD, NE, CMR, IOL, and OVD. For the purpose of comparing the SCM completion time to the completion time of an equivalent manual surgery, the following steps were omitted as their durations were not recorded across both cases: VIS, PRO, No Activity, Paracentesis, General Injection, Capsulorhexis Initiation, Capsulorhexis Formation, and Wound Hydration. - Figure 7c. The completion time of an SCM case (7:09) is comparable to that in the BigCat database (7:46).

SCM Case Surgical Step	INC	HYD	NE-SCM	CMR	IOL	OVD
Equivalent Step in BigCat Database	Main Wound	Hydrodissection	Phacoemulsification	Cortical Removal	Lens Insertion	Viscoelastic Removal

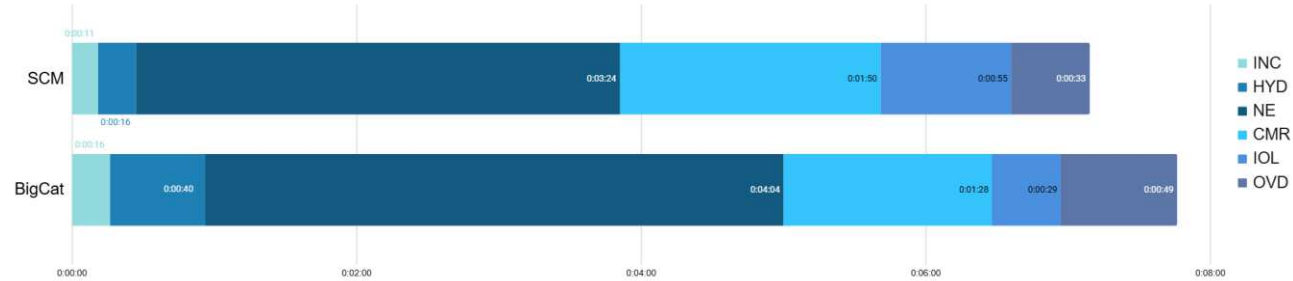
Table 5: SCM Case and BigCat Database Equivalent Surgical Steps



(a)



(b)



(c)

Figure 7: Time analysis of the surgical procedure; acronyms defined in Table 2. (a) Statistics of the intraocular completion time for the individual surgical steps of the cataract procedure - Box plots of Polaris-performed intraocular surgical steps. (b) The Duration of

Polaris Surgical Steps as a Percentage of the Total Polaris Intraocular Time Compared Between SCM Cases on Average and SCM + SSM Cases on Average (c) Polaris Intraocular Durations Broken Down by Surgical Step Compared Between the SCM Case With the Shortest Polaris Intraocular Duration (Subject 110 - Total intraocular time: 7:28) and the Average Duration of Surgical Steps in Manual Cataract Surgery According to the BigCat Database.

4. Conclusions & Discussion

This study presented the world's first-in-human cataract surgery evaluating the Polaris surgical robotic system (Horizon Surgical Systems Inc., Malibu, CA) while demonstrating its feasibility, safety, and early clinical effectiveness. Polaris was designed with a workspace enabling accurate and precise positioning and orientation of surgical instruments throughout the entire intraocular anatomy; cataract surgery was therefore selected as the initial clinical indication for system validation. Across a cohort of 10 subjects, Polaris successfully completed all steps of the cataract procedure with robotic assistance, with the exception of the capsulorhexis, which was performed using a femtosecond laser platform (LENSAR).

The study includes two modes of operation: Surgeon Control Mode (SCM) and Surgeon Supervised Mode (SSM), the latter incorporating autonomous execution of partial nucleus extraction using phacoemulsification. The results demonstrated that both modes achieved the expected safety levels and clinical performance outcomes, with no intraoperative adverse events reported. Postoperative visual acuity outcomes at 90 days were as expected following a premium treatment, with nearly 20/20 vision achieved in the 9 out of the 10 subjects and 20/25 in one case. Furthermore, intraocular procedure times in SCM were comparable to those reported for manual techniques, as benchmarked against the BigCat database.

The introduction of autonomous operation (SSM) represents a significant advancement in ophthalmic surgical robotics. These findings support the hypothesis that the eye—despite being composed of soft tissue—can be treated as a sufficiently structured environment to enable autonomous intervention. Moreover, the study demonstrates that an AI-driven control system, leveraging intraoperative OCT in conjunction with digital microscopy, can perform autonomous actions while maintaining the high levels of accuracy and precision required in ophthalmic surgery.

More broadly, surgical robotics in general and in particular autonomous operation as demonstrated in this study, impacts the three foundational pillars of surgery:
(1) **Surgeon** – enhancing sensing (advanced visualization), action (precision, accuracy, dexterity), and cognition (decision support); (2) **Patient** – improving access to care and enabling superior clinical outcomes; (3) **Healthcare systems** – increasing procedural throughput and efficiency, thereby addressing the growing mismatch between patient demand and the availability of trained surgeons.

Statements

Human Ethics and Consent to Participate declaration:

All subjects participating in this study signed an informed consent. The study was approved by the Comite Nacional de Etica de la Investigacion en Salud El Salvador (National Ethics Committee on Health Research, El Salvador) for experimental protocol no. HS-001 following all the guidance and regulation. The trial was initially registered at ClinicalTrials.gov (NCT 06990074) on 06 MAY 2025

Competing Interest declaration

Jacob Rosen – Is a Professor at UCLA and Horizon Surgical Systems Employee

Pooria Kashani, Matt Gerber, Petra Stepke, Peter Walker Ferguson, Changyeob Shin, Alexandre Tiard, Al-Hafeez Dhalla, Mitchell Harris, Eric Peltola, Hai Bui, Hyoenmu Yoo, Rajesh Rajpal, Jean-Pierre Hubschman – Are Horizon Surgical Systems Employees

Tsu-Chin Tsao - Is a Professor UCLA and a UCLA employee. He is also the Chair of the Scientific board at Horizon Surgical System (Unpaid)

David Lozano - Is a Professor at UCLA, a UCLA employee, and a consultant for Horizon Surgical Systems (paid)

Steve Schwartz – Is an ophthalmic surgeon in privet practice and a board member at Horizon Surgical Systems (unpaid)

Uday Devgan - Is an ophthalmic surgeon in privet practice and a clinical advisory board member at Horizon Surgical Systems (unpaid)

Firas Rahhal - Is an ophthalmic surgeon in privet practice and a board member at Horizon Surgical Systems (unpaid)

Richard L. Lindstrom - Is an ophthalmic surgeon in privet practice and the head of the clinical advisory board at Horizon Surgical Systems (unpaid)

Data Availability Declaration

There is additional available data beyond the numerical data included in this manuscript

Funding Declaration

The activity reported in this study was supported by private funding. No federal funding was used

Author Contribution Declaration

Jacob Rosen – As the lead co-author he directed the engineering aspects of the system development, directed the data collection followed by their analysis, and co-authored the paper.

Pooria Kashani, Peter Walker Ferguson, Changyeob Shin, Alexandre Tiard, Al-Hafeez Dhalla, Mitchell Harris, Eric Peltola, Hai Bui, Hyoenmu Yoo, Tsu-Chin Tsao David Lozano, Steve Schwartz, Uday Devgan, Firas Rahhal, Richard L. Lindstrom, Jean-Pierre Hubschman – As co-authors they were involved in co-leading the system development, defining and executing the experimental protocol, and performing the post processing data analysis.

Matt Gerber - As co-author he was involved in the system development, defining and executing the experimental protocol, and performing the post processing data analysis of the OCT.

Petra Stepke - As co-author she was involved in providing technical clinical support to the system, and performing the post processing surgical execution time analysis.

Rajesh Rajpal - As the lead co-author he was involved in collecting and analyzing the pre and post clinical testing of the subjects.

References

[1] Asbell PA, et al. Age-related cataract. *The Lancet*. 2005;365(9459):599–609.

[2] Chen X, Woreta FA, Chang JR. Cataract: epidemiology, pathophysiology, and global burden. *JAMA*. 2025.

[3] Pascolini D, Mariotti SP. Global estimates of visual impairment: 2010. Br J Ophthalmol 2012;96:614–8.

[4] Yorston D, Wood M, Foster A. *Visual outcomes of cataract surgery: a review.* Br J Ophthalmol. 2024;108(3):300–310.2

[5] Chen SP, Woreta FW, Chang DF. *Cataracts: A Review.* JAMA. 2025;333(6):567–576.1

[6] Gogate P, et al. *Cataract surgical outcomes and associated factors in low- and middle-income settings: a systematic review.* Trop Ophthalmol. 2024;54(4):12–20.3

[7] Yorston D, Wood M, Foster A. *Visual outcomes of cataract surgery: a review.* Br J Ophthalmol. 2024;108(3):300–310.2

[8] Chen SP, Woreta FW, Chang DF. *Cataracts: A Review.* JAMA. 2025;333(6):567–576.1

[9] Gogate P, et al. *Cataract surgical outcomes and associated factors in low- and middle-income settings: a systematic review.* Trop Ophthalmol. 2024;54(4):12–20.3

[10] Arun J Thirunavukarasu, Monica L Hu , William P Foster, Kanmin Xue, Jasmina Cehajic-Kapetanovic, Robert E MacLaren, Robot-Assisted Eye Surgery: A Systematic Review of Effectiveness, Safety, and Practicality in Clinical Settings

[11] G. S. Guthart and J. K. Salisbury Jr., “The Intuitive™ telesurgery system: Overview and application,” *Proc. IEEE Int. Conf. Robotics and Automation (ICRA)*, 2000, pp. 618–621.

[12] P. Dupont, et al., “A decade retrospective of medical robotics research from 2000 to 2010,” *IEEE Trans. Robotics*, vol. 29, no. 6, pp. 1357–1372, 2013.

[13] R. H. Taylor and D. Stoianovici, “Medical robotics in computer-integrated surgery,” *IEEE Trans. Robotics and Automation*, vol. 19, no. 5, pp. 765–781, 2003.

[14] Jacob Rosen, Blake Hannaford, Richard Satava, Surgical Robotics – Systems Applications and Visions, 1st edition 2011 by Springer US, ISBN 978-1-4419-1126-1

[15] A. Lanfranco, A. E. Castellanos, J. P. Desai, and W. C. Meyers, “Robotic surgery: A current perspective,” *Annals of Surgery*, vol. 239, no. 1, pp. 14–21, 2004.

[16] Jacob Rosen et al., Raven: Developing a Surgical Robot from a Concept to a Transatlantic Teleoperation Experiment, Chapter 8 in Surgical Robotics, Systems, Applications, and Visions, Jacob Rosen, Blake Hannaford, Richard M. Satava (Editors), 1 ed. Springer 2011.

[17] R. H. Taylor, P. Jensen, L. L. Whitcomb, A. Barnes, R. Kumar, D. Stoianovici, et al., “A steady-hand robotic system for microsurgical augmentation,” *Int. J. Robotics Research*, vol. 18, no. 12, pp. 1201–1210, 1999.

[18] B. J. Fregly, S. Rahman, and W. E. Banks, “Theoretical accuracy of a universal surgical robot for total hip replacement,” *Clinical Orthopaedics and Related Research*, vol. 405, pp. 209–220, 2002.

[19] M. T. K. Jensen, I. T. Todorov, and E. Vander Poorten, “Toward intraoperative imaging-guided robotic interventions: A review,” *IEEE Rev. Biomedical Engineering*, vol. 10, pp. 261–280, 2017

[20] M. J. Edwards, G. T. Bourges, and R. E. MacLaren, “Ophthalmic surgical robotics: Applications and future directions,” *Eye*, vol. 32, no. 2, pp. 237–245, 2018.

[21] Matthew J. Gerber, Moritz Pettenkofer, Jean-Pierre Hubschman, Advanced robotic surgical systems in ophthalmology, Eye (2020) 34:1554–1562

[22] Abadi AS, Ordys A, Kukielka K, Pierscionek B. “Review on challenges for robotic eye surgery; surgical systems, technologies, cost-effectiveness, and controllers.” *Int J Med Robot.* 2023;19(4):e2524.

[23] de Smet MD, Naus GJ, Faridpooya K, Mura M. “Robotic-assisted surgery in ophthalmology.” *Curr Opin Ophthalmol.* 2018;29(3):248–253

[24] Alafaleq M. Robotics and cybersurgery in ophthalmology: a current perspective. J Robot Surg. 2023 Aug;17(4):1159-1170.

[25] R. A. MacLachlan, B. C. Becker, J. Cuevas Tabarés, G. W. Podnar, L. A. Lobes Jr., and C. N. Riviere, “Micron: An Actively Stabilized Handheld Tool for Microsurgery,” IEEE Transactions on Robotics, **vol. 28, no. 1, pp. 195–212, 2012. doi:10.1109/TRO.2011.2169634

[26] Alireza Alamdar, David E. Usevitch, Jiahao Wu, Russell H. Taylor, Peter Gehlbach, Iulian Iordachita Steady-Hand Eye Robot 3.0: Optimization and Benchtop Evaluation for Subretinal Injection, IEEE Trans. Medical Robotics and Bionics, 2024.

[27] Jason T. Wilson, et al. Intraocular robotic interventional surgical system (IRISS): Mechanical design, evaluation, and master–slave manipulation, Int J Med Robotics Comput Assist Surg. 2018;14

[28] Cheng-Wei Chen et. al, Intraocular robotic interventional surgical system (IRISS): Semi-automated OCT-guided cataract removal. The international journal of medical robotics + computer assisted surgery : MRCAS, 14(6), 2018

[29] Anibal Francone; Jason Mingyi Huang; Ji Ma; Tsu-Chin Tsao; Jacob Rosen; Jean-Pierre Hubschman, The Effect of Haptic Feedback on Efficiency and Safety During Preretinal Membrane Peeling Simulation, Translational Vision Science & Technology July 2019, Vol.8, 2.

[30] Matthew J. Gerber, Jean-Pierre Hubschman, Tsu-Chin Tsao, Robotic posterior capsule polishing by optical coherence tomography image guidance, Int J Med Robot. 2021;17

[31] Gerber, Matthew J; Hubschman, Jean-Pierre; Tsao, Tsu-Chin, Automated Retinal Vein Cannulation on Silicone Phantoms Using Optical-Coherence-Tomography-Guided Robotic Manipulations, IEEE/ASME transactions on mechatronics. , 2021, Vol.26(5), p.2758-2769

[32] Changyeob Shin , Matthew J. Gerber , Yu-Hsiu Lee , Mercedes Rodriguez, Sahba Aghajani Pedram, Jean-Pierre Hubschman, Tsu-Chin Tsao , and Jacob Rosen, Semi-Automated Extraction of Lens Fragments Via a Surgical Robot Using Semantic Segmentation of OCT Images With Deep Learning - Experimental Results in Ex Vivo Animal Model, IEEE robotics & automation letters. , 2021, Vol.6(3), p.5261-5268

[33] Sahba Aghajani Pedram, Peter W. Ferguson, Matt J. Gerber, Jean-Pierre Hubschman, Jacob Rosen, A Novel Tissue Identification Framework in Cataract Surgery using an Integrated Bioimpedance-Based Probe and Machine Learning Algorithms, IEEE Transactions on Biomedical Engineering (TBME) - IEEE TRANSACTIONS ON BIOMEDICAL ENGINEERING, VOL. 69, NO. 2, FEBRUARY 2022

[34] Yu-Hsiu Lee, Yu-Ting Lai , Matthew J. Gerber , Jaime Dodds, Jean-Pierre Hubschman, Jacob Rosen , and Tsu-Chin Tsao, Accurate Robotic Posterior Capsule Polishing With Tissue Stabilization, IEEE/ASME TRANSACTIONS ON MECHATRONICS, VOL. 29, NO. 1, FEBRUARY 2024

[35] YI Leiderman, MJ Gerber, JP Hubschman, D Yi, Artificial intelligence applications in ophthalmic surgery Current Opinion in Ophthalmology, Vol.35, Issue 6, 2024

[36] T. L. Edwards, K. Xue, H. C. M. Meenink, et al., “First-in-human study of the safety and viability of intraocular robotic surgery,” *Nat. Biomed. Eng.*, vol. 2, pp. 649–656, 2018.

[37] Cehajic-Kapetanovic J, Xue K, Edwards TL, Meenink TC, Beelen MJ, Naus GJ, de Smet MD, MacLaren RE. First-in-Human Robot-Assisted Subretinal Drug Delivery Under Local Anesthesia. American Journal of Ophthalmology. 2022;237:104–113.

[37] https://www.acusurgical.com

[38] Ossama Mahmoud, Han Zhang, Nicholas Matton, Shahzad I. Mian, Bradford Tannen, Nambi Nallasamy, CatStep: Automated Cataract Surgical Phase Classification and Boundary Segmentation Leveraging Inflated 3D-Convolutional Neural Network Architectures and BigCat, Ophthalmology Science Volume 4, Number 1, February 2024

[30] Trikha S, Agrawal S, Saffari SE, Jayaswal R, Yang YF. Visual outcomes in patients with zonular dialysis following cataract surgery. Eye (Lond). 2016 Oct;30(10):1331-1335.

[40] Pricopie S, Istrate S, Voinea L, Leasu C, Paun V, Radu C. Pseudophakic bullous keratopathy. Rom J Ophthalmol. 2017 Apr-Jun;61(2):90-94.

[41] Kim JY, Jo MW, Brauner SC, Ferrufino-Ponce Z, Ali R, Cremers SL, Henderson BA. Increased intraocular pressure on the first postoperative day following resident-performed cataract surgery. Eye (Lond). 2011 Jul;25(7):929-36.

[42] Chu CJ, Johnston RL, Buscombe C, Sallam AB, Mohamed Q, Yang YC; UK Pseudophakic Macular Edema Study Group. Ophthalmology. 2016;123(2):316–323.

[43] S. A. Boppart, B. E. Bouma, C. Pitris, G. J. Tearney, J. F. Southern, M. E. Brezinski, and J. G. Fujimoto, “Intraoperative assessment of microsurgery with three-dimensional optical coherence tomography,” Radiology 208(1), 81–86 (1998).

[44] Y. K. Tao, J. P. Ehlers, C. A. Toth, and J. A. Izatt, “Intraoperative spectral domain optical coherence tomography for vitreoretinal surgery,” Opt. Lett. 35(20), 3315–3317 (2010).

[45] Carrasco-Zevallos, Oscar M., Christian Viehland, Brenton Keller, Mark Draelos, Anthony N. Kuo, Cynthia A. Toth, and Joseph A. Izatt. "Review of intraoperative optical coherence tomography: technology and applications." Biomedical optics express 8, no. 3 (2017): 1607-1637.